

Article

Risk Assessment and Analysis of Rock Burst under High-Temperature Liquid Nitrogen Cooling

Yuhe Cai ^{1,2}, Yankun Ma ^{3,*}, Teng Teng ⁴ , Yi Xue ¹, Linchao Wang ¹, Zhengzheng Cao ^{2,*} and Zhizhen Zhang ⁵ ¹ School of Civil Engineering and Architecture, Xi'an University of Technology, Xi'an 710048, China² International Joint Research Laboratory of Henan Province for Underground Space Development and Disaster Prevention, Henan Polytechnic University, Jiaozuo 454000, China³ Scientific and Technological Research Platform for Disaster Prevention and Control of Deep Coal Mining, Anhui University of Science and Technology, Huainan 232001, China⁴ School of Energy and Mining Engineering, China University of Mining and Technology-Beijing, Beijing 100083, China⁵ School of Mechanics and Civil Engineering, China University of Mining and Technology, Xuzhou 221116, China

* Correspondence: mayankun2008@126.com (Y.M.); caozz2008@126.com (Z.C.)

Abstract: Rock burst, an important kind of geological disaster, often occurs in underground construction. Rock burst risk assessment, as an important part of engineering risk assessment, cannot be ignored. Liquid nitrogen fracturing is a new technology used in the geological, oil, and gas industries to enhance productivity. It involves injecting liquid nitrogen into reservoir rocks to induce fractures and increase permeability, effectively reducing rock burst occurrences and facilitating the flow of oil or gas toward the wellbore. The research on rock burst risk assessment technology is the basis of reducing rock burst geological disasters, which has important theoretical and practical significance. This article examines the temperature treatment of two types of rocks at 25 °C, 100 °C, 200 °C, 300 °C, and 400 °C, followed by immersion in a liquid nitrogen tank. The temperature difference between the liquid nitrogen and the rocks may trigger rock bursting. The research focused on analyzing various characteristics of rock samples when exposed to liquid nitrogen. This included studying the stress–strain curve, elastic modulus, strength, cross-section analysis, wave velocity, and other relevant aspects. Under the influence of high temperature and a liquid nitrogen jet, the wave velocity of rocks often changes. The structural characteristics and possible hidden dangers of rocks can be understood more comprehensively through section scanning analysis. The stress–strain curve describes the deformation and failure behavior of rocks under different stress levels, which can help to evaluate their stability and structural performance. The investigation specifically focused on the behavior of rocks subjected to high temperatures and liquid nitrogen. By analyzing the stress–strain curves, researchers were able to identify the precursors and deformation processes that occur before significant deformation or failure. These findings have implications for the mechanical properties and stability of the rocks.

Keywords: liquid nitrogen; rock burst; temperature; wave velocity; strength; section

Citation: Cai, Y.; Ma, Y.; Teng, T.; Xue, Y.; Wang, L.; Cao, Z.; Zhang, Z. Risk Assessment and Analysis of Rock Burst under High-Temperature Liquid Nitrogen Cooling. *Water* **2024**, *16*, 516. <https://doi.org/10.3390/w16040516>

Academic Editors: Helena M. Ramos and Perrin Jerome

Received: 7 January 2024

Revised: 26 January 2024

Accepted: 1 February 2024

Published: 6 February 2024



Copyright: © 2024 by the authors. Licensee MDPI, Basel, Switzerland. This article is an open access article distributed under the terms and conditions of the Creative Commons Attribution (CC BY) license (<https://creativecommons.org/licenses/by/4.0/>).

1. Introduction

Rock burst is an important geological hazard that often occurs during underground construction [1–3]. At the same time, geothermal resources are being vigorously developed. Geothermal resources are widely distributed in sedimentary basins, volcanic areas, hydrothermal areas, geothermal systems, and other areas around the world, and are regarded as a clean, efficient, and reliable source of energy. Compared with other heating methods, geothermal heating has the advantages of environmental protection, stability, being economical, and having significant energy-saving effects. China has enormous potential for deep geothermal energy resources, so exploring the use of deep geothermal energy

is of great significance [4–6]. In the future, the development of geothermal energy will tend to develop and utilize deep geothermal energy and high-temperature magma energy and gradually focus on the comprehensive utilization of geothermal heating, refrigeration, hot springs, and bathhouses [7–10]. Therefore, the safety of underground engineering should be given special attention. Currently, engineering cases have shown that rock burst accidents can affect the normal operation and basic life and property safety of construction projects [11–15]. Therefore, rock burst risk assessment, as an important component of engineering risk assessment, can no longer be ignored, and the research on rock burst risk assessment technology has important theoretical and engineering practical significance. Liquid nitrogen, as a new means of stimulating rocks, may induce rock bursts. When rocks come into contact with liquid nitrogen, in addition to the pressure of the liquid itself, the temperature difference between the two can generate considerable temperature stress, causing thermally induced cracks on the surface of the rocks, which can induce rock bursts [16–19]. Currently, assessing the rock burst risk of rocks typically involves a combination of laboratory and field tests. Certainly, numerical simulation methods play a crucial role in assessing the rock burst risk of rocks. These methods offer several advantages in accurately predicting parameters, such as stress, deformation, temperature, and moisture in rocks, which are essential for evaluating the potential for rock bursts. This study evaluates and analyses the rock burst risk of rocks under the action of liquid nitrogen, grading safety risks according to the damage mechanism of liquid nitrogen to rocks, the probability of rock burst occurrence, and the level of loss. By combining appropriate risk management methods and regulations with the use of liquid nitrogen, a comprehensive approach to managing rock burst risk can be achieved. Liquid nitrogen injection is a technique that involves the controlled injection of liquid nitrogen into rock masses to mitigate the risk of rock bursts.

The criteria and classification methods in rock burst research are important tools for assessing the rock burst hazard of rocks. By monitoring and analyzing the deformation and stress state of rocks, early signs of rock bursts can be detected. Rock burst prevention and control are crucial aspects of rock burst research [20–26]. Liquid nitrogen, as a low-temperature treatment method, can be used for modification and freezing treatment of rocks [27–32]. Research has indicated that the mechanical properties of rocks can be noticeably diminished through the application of liquid nitrogen freezing, and the sensitivity to this freezing method varies depending on the water content and rock type. Particularly, saturated rocks are more significantly affected. The thermal shock effect of liquid nitrogen can cause shrinkage deformation and reduced pore volume in dry rocks [33,34]. When liquid nitrogen infiltrates the pores and fractures of rocks and forms ice crystals, the expansion of water during the freezing process can generate stress within the rocks, leading to damage and fracture at weakly bonded mineral particle interfaces and potentially causing fractures through propagation. In summary, liquid nitrogen has potential applications in rock burst research. However, specific rock burst risk assessment and liquid nitrogen freezing treatments need to consider factors, such as different rock types and water contents, and laboratory and field tests are necessary to validate the results. Scientifically reasonable evaluation and decision-making based on relevant regulations and standards are also required for the safe use of liquid nitrogen and the development of rock burst prevention and control measures.

Currently, rock bursts cause huge damage to engineering projects, with strong destructive force and limited prevention and control methods. At the same time, there are also imperfections in the risk assessment system. To address this issue, investigations have been carried out on the development of a risk assessment system for rock bursts, including the following main aspects: data obtained through uniaxial compression tests, acoustic emission tests, ultrasonic detection tests, and rock sample section scanning can provide relevant information on rock bursts. These data can reveal the mechanical properties of rocks, stress concentration areas, crack propagation, and the interaction between rocks and liquid nitrogen. At the same time, the results of acoustic waves and section scanning can

show the internal situation and changes in rocks. During the experimental process, the experimental plan is optimized, and improvement measures are proposed according to the actual situation. The aim of these research efforts is to enhance the dependability and precision of the findings [35]. Finally, through the processing and analysis of experimental data, the performance of rocks under the action of high-temperature liquid nitrogen can be deeply studied, providing an important reference for optimizing high-temperature liquid nitrogen fracturing technology, evaluating rock stability, and guiding the development of geothermal resources. These research results are of great significance for improving the rock burst risk assessment system, improving rock burst prevention and control methods, and enhancing engineering safety.

2. Experimental Equipment and Experimental Process

2.1. Experimental Materials

The studied granite is a common reservoir rock type in the EGS and is taken from Xuzhou, Jiangsu. It is coarse-grained and uniform, with a distinctive light brown color. According to the recommendations of ISRM, standard cylindrical specimens should be prepared from a single rock block to maintain the uniformity of the specimens.

2.2. Experimental Methods and Equipment

The main equipment used in this experiment includes the domestically produced TAWD-2000 electro-hydraulic servo rock mechanics testing system (Changchun Chaoyang Testing Instrument Co., Ltd., Changchun, China) for uniaxial compression experiments. This system can perform various tests, such as uniaxial, triaxial, direct shear, and creep on rocks, and can calculate various mechanical parameters of rocks. As depicted in Figure 1a, the system comprises three main components: an axial loading system, a computer control system, and a confining pressure loading system. The axial ultimate load capacity of the system is 2000 kN, the confining pressure range spans from 0 to 80 MPa, and the frame stiffness is 500 tf/mm. The axial displacement measurement range is 0–100 mm with an accuracy of $\pm 0.5\%$, and the circumferential displacement measurement range is 0–5 mm with an error of $\pm 0.3\%$. The control modes mainly include stress control, strain control, and displacement control, with seamless switching between different control modes. This system can provide a maximum pressure peak of 20 kN and offers high control precision. Pre-stressing is not required during the testing process, and it can automatically reset the contact force and displacement, enabling the acquisition of precise load displacement curves. Additionally, there is a liquid nitrogen tank for cooling rock samples, as shown in Figure 1b; a PIC-2 acoustic emission control and acquisition system for monitoring acoustic emission signals, with a frequency monitoring range of 1 kHz to 3 MHz, as shown in Figure 1c; an NM-4A non-metallic ultrasonic detection instrument for analyzing internal defects in granite samples, as depicted in Figure 1d; and a VR-5000 three-dimensional surface profiler for analyzing the fracture surface morphology characteristics of granite specimens, as shown in Figure 1e.



Figure 1. Experimental apparatus.

2.3. Protocol and Procedure

Divide the samples into untreated at 25 °C and 25 °C + LN₂, heating to 100 °C + LN₂, heating to 200 °C + LN₂, heating to 300 °C + LN₂, and heating to 400 °C + LN₂. There will be two samples for each condition labeled as follows: 25-1 untreated, 25-2 untreated, 100-1, 100-2, 200-1, 200-2, 300-1, 300-2, 400-1, and 400-2. The granite sample is shown in Figure 2. High-temperature heating refers to heating the sample to the set temperature and then continuing to heat for 3 h to ensure that the inside and outside of the rock sample reach the set temperature. The high temperature will be set at 300 °C, and no heating will be performed for the room temperature group. Liquid nitrogen cooling refers to completely immersing the heated rock sample in a liquid nitrogen container for three hours. At the same time, the rock heated after will be placed in the liquid nitrogen container, and the rock sample will boil with the liquid nitrogen, so the liquid nitrogen should not be filled too full. After the cooling is completed, the next step of the experiment will be conducted.



Figure 2. Granite specimens.

3. Uniaxial Compression Test and Rock Burst Tendency Determination

3.1. Mechanical Properties Curve

3.1.1. Stress–Strain Curve

The stress–strain curve is a fundamental tool used to comprehend the mechanical response of rocks when subjected to external forces. It provides valuable insights into the strength characteristics, deformation behavior, and stability evaluation of rock in various environmental conditions. One key aspect revealed by the stress–strain curve is the strength characteristics of the rock. By analyzing this curve, we can determine important parameters such as the maximum bearing capacity, plastic deformation characteristics, and failure mode of the rock. This information is crucial for engineering designs involving rock masses, as it helps ensure structural stability and safety. Moreover, the stress–strain curve also sheds light on the deformation behavior of rock. It captures the elastic deformation and plastic deformation of the rock, offering insights into the underlying deformation mechanisms and characteristics. Understanding these behaviors is essential for predicting and managing the response of rock formations to external loads, such as those induced by mining or civil engineering activities.

Absolutely, the stress–strain curve is crucial for evaluating the stability and seismic performance of rock. By analyzing this curve, researchers and engineers can assess the potential for rock mass instability, identify critical failure points, and design appropriate mitigation measures. This information is particularly valuable in geotechnical engineering projects, where accurate stability evaluations are essential for ensuring the integrity and safety of structures built on or within rock formations. Figure 3 shows the stress–strain curves at different temperatures under uniaxial compression. In the specific case of granite, the stress–strain curve exhibits four distinct phases: the compaction phase, elastic deformation phase, plastic deformation phase, and ultimate failure phase. During the compaction phase, the physical and mechanical characteristics of the rock deteriorate due to the presence of microscopic structures like pores, cracks, and joints. As the applied load progressively rises, the rock transitions into the elastic deformation phase, where it exhibits linear elastic properties with minimal changes in its microstructure.

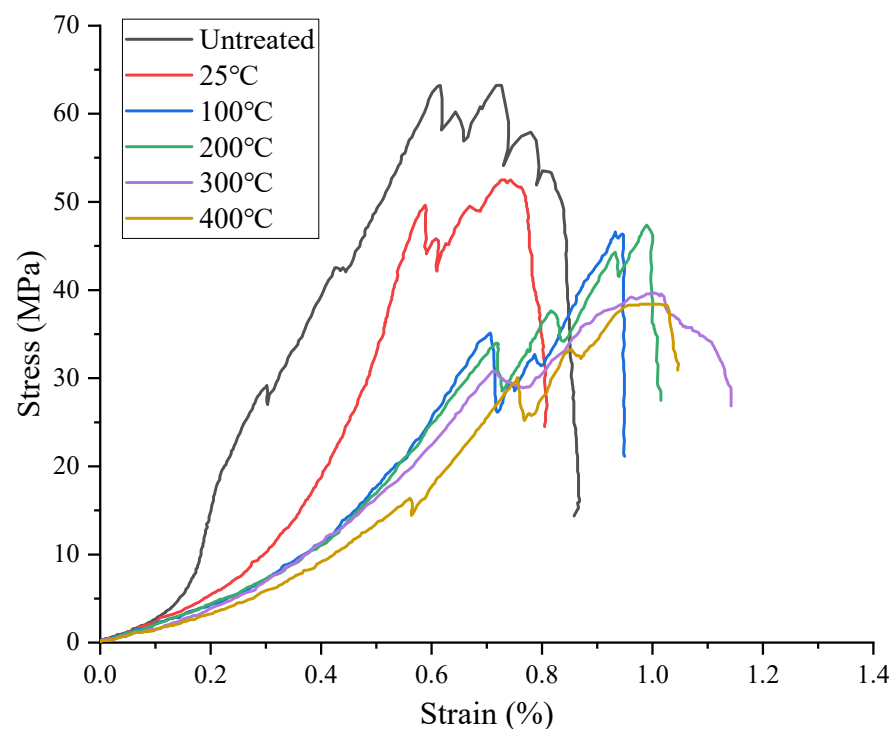


Figure 3. Stress–strain curves at different temperatures under uniaxial compression.

Upon further loading, the rock enters the yielding stage characterized by stable crack extension. During this stage, the rate of crack extension exceeds the closure rate, leading to a gradual decrease in strength. Finally, in the failure stage, cracks propagate and intensify until the loading stress reaches its peak strength. At this point, the specimen experiences instantaneous splitting or bursting failure, resulting in a sharp decrease in axial stress. It is worth noting that the stress–strain curve of rock can be influenced by various factors, such as temperature and cooling methods. Under compressive loading, micro-pores and cracks tend to close. However, the specific characteristics of the stress–strain curve may vary depending on the thermal conditions and cooling techniques employed. Understanding these variations is crucial for accurately predicting and managing the mechanical behavior of rock in different environmental contexts. In conclusion, the stress–strain curve of rock provides a wealth of information regarding its strength characteristics, deformation behavior, and stability evaluation. By comprehensively analyzing this curve and considering the influence of external factors, engineers and researchers can make informed decisions when designing structures and managing rock formations in diverse geotechnical projects.

The use of liquid nitrogen treatment on rock samples has been observed to affect their mechanical behavior, particularly during the compaction, elastic, and failure stages. Treated samples exhibit distinct characteristics compared to untreated ones, indicating the influence of this cooling technique on the rock's response to external forces. During the compaction stage, it has been noted that rock samples treated with liquid nitrogen display a faster strain increase rate and non-linear growth. This phenomenon can be attributed to the presence of increased internal cracks caused by the liquid nitrogen treatment. These cracks make the sample more susceptible to plastic deformation under stress, leading to the observed non-linear behavior. The enhanced crack density may result from the thermal shock induced by the rapid cooling process.

Interestingly, when examining the relationship between the compaction stage curve and heating temperature in the same rock samples treated with liquid nitrogen, no apparent linear relationship is observed. This suggests that the heating temperature has little influence on the behavior of the rock during this stage. Other considerations, such as the chemical and physical characteristics of the samples and the cooling treatment temperature, might play a more significant role in determining their compaction behavior. Moving to the elastic stage, it has been observed that the slope of the stress–strain curve for samples treated with liquid nitrogen decreases with increasing temperature. This indicates that the treatment weakens the load-bearing capacity of the rock, particularly at higher cooling temperatures. The cooling process might induce structural changes in the rock, affecting its ability to withstand stress. Further studies are needed to fully understand the underlying mechanisms responsible for this temperature-dependent behavior. In the failure stage, the ductility of rock samples treated with liquid nitrogen shows some enhancement. This could be attributed to the treatment's ability to suppress crack propagation within the rock. By effectively controlling the growth and extension of cracks, the toughness of the rock is increased, resulting in improved ductility. This finding suggests that liquid nitrogen treatment might have potential applications in enhancing the fracture resistance of rock materials.

In summary, liquid nitrogen treatment has been observed to exert a significant influence on the compaction and elastic stages of rock samples. The treatment affects the strain increase rate, non-linear growth, load-bearing capacity, and ductility of the rock. However, its impact on the failure stage appears to be relatively smaller. Further research is required to fully elucidate the specific influencing factors, including the chemical and physical characteristics of the samples and the cooling treatment temperature. Understanding these effects will contribute to the development of more accurate models and predictive tools for assessing the behavior of rock subjected to different cooling techniques.

3.1.2. Elastic Modulus and Compressive Strength

Furthermore, the findings depicted in Figure 4 also demonstrate that the application of liquid nitrogen treatment significantly affects the compressive strength of rock specimens at different heating temperatures. The observed fluctuations in compressive strength suggest that the cooling treatment affects the internal structure and composition of the rock, leading to changes in its mechanical properties. Specifically, for samples treated with liquid nitrogen, a decrease in compressive strength is observed at 100 °C and 200 °C, which suggests a reduction in the load-bearing capacity of the rock. This could be attributed to the thermal shock induced by the cooling process, which might cause microcracks or other defects within the rock. As the temperature increases to 300 °C, there is a certain degree of increase in compressive strength. This suggests that the cooling treatment could induce a rearrangement of the crystal structure or enhance the interparticle bonding, resulting in an improvement in the rock's resistance to failure. Interestingly, at 400 °C, there is a further increase in compressive strength, which may indicate the presence of a critical point or threshold temperature; beyond this point, the mechanical properties of the rock undergo significant alterations. This observation highlights the importance of considering the specific cooling treatment conditions when evaluating the impact of liquid nitrogen treatment on the compressive strength of rock samples.

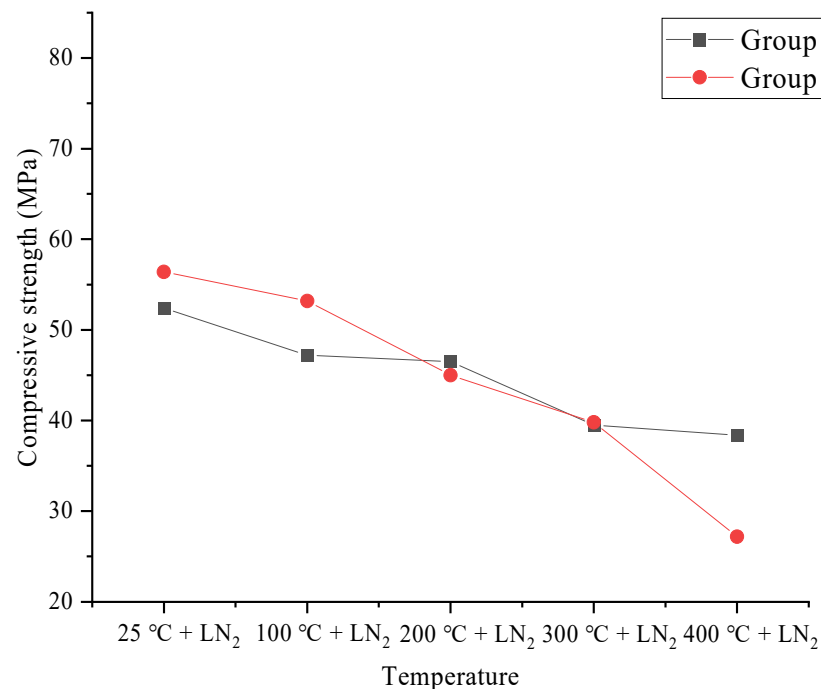


Figure 4. Evolution trend of compressive strength with temperature.

Overall, these findings suggest that liquid nitrogen treatment can induce significant changes in the compressive strength of rock samples, particularly at different heating temperatures. The observed fluctuations and sudden changes in rate could be attributed to the complex interactions between the cooling treatment and the internal structure of the rock. Additional research is required to comprehensively comprehend the underlying mechanisms accountable for these effects and to devise more effective methodologies to enhance the mechanical properties of rocks exposed to various cooling techniques.

In Figure 5, it is evident that as the treatment temperature increases, the elastic modulus of the rock generally shows a non-linear decreasing trend, except for group 1, where there is a slight increase in elastic modulus at 200 °C and a sharp change in elastic modulus after the temperature rises to 200 °C. Both samples exhibit this trend, with the elastic modulus of group 1 decreasing from 60.15 MPa to 42.22 MPa and the elastic modulus of group 2

decreasing from 43.98 MPa to 25.82 MPa. This indicates that the greater the temperature difference during liquid nitrogen treatment, the greater the change in elastic modulus, indicating that temperature affects the ability of liquid nitrogen to resist rock failure, which is basically an increasing trend.

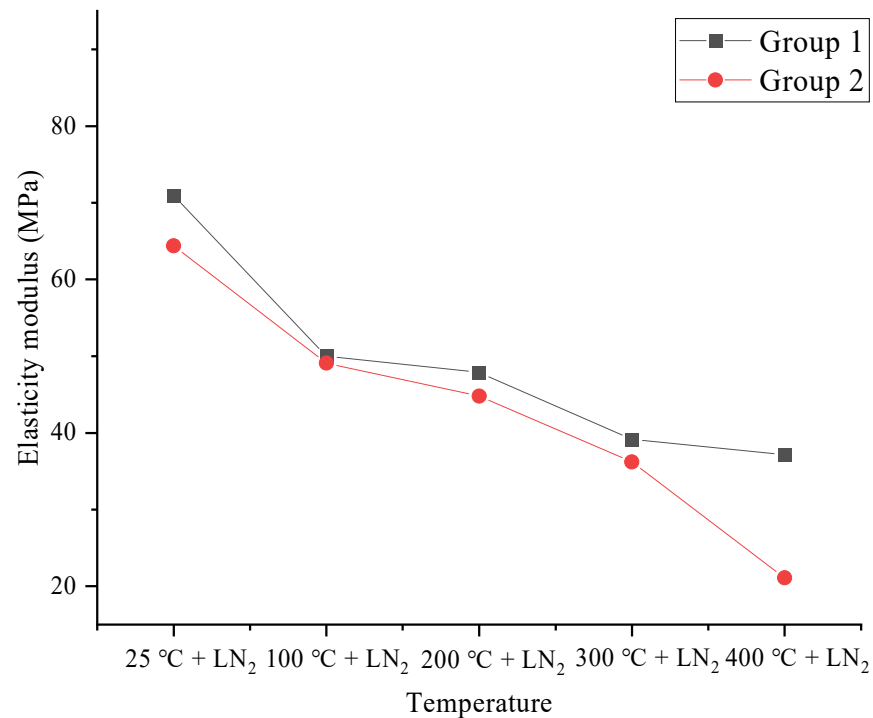


Figure 5. Evolution trend of modulus of elasticity with temperature.

3.2. Determination of Rock Burst Propensity

In this section, based on the previously acquired data, an investigation into the proneness of granite rock to rock bursts is conducted. The elastic strain energy index is utilized to assess the susceptibility of the temperature granite to rock bursts. The susceptibility to rock bursts is determined by the ratio W of the elastic strain energy stored within the rock to the dissipated strain energy. Based on the computed outcomes, the proneness of the rock-to-rock bursts can be classified into four levels: no proneness, weak proneness, moderate proneness, and strong proneness. These four levels serve as criteria for rock burst assessment. This study focuses on the rock burst proneness of granite specimens subjected to different numbers of liquid nitrogen treatments during the process of deformation and failure of the rock mass. The calculation formula for W is as follows:

$$W = \frac{U_e}{U_d} \quad (1)$$

where U_e denotes the elastic strain energy and U_d represents the dissipated strain energy. The calculation approach involves integrating the area under the curve prior to the peak load to determine the elastic strain energy and integrating the area under the curve following the peak load to determine the dissipated strain energy. The trends of elastic strain energy and dissipative strain energy with temperature variations are shown in Figures 6 and 7.

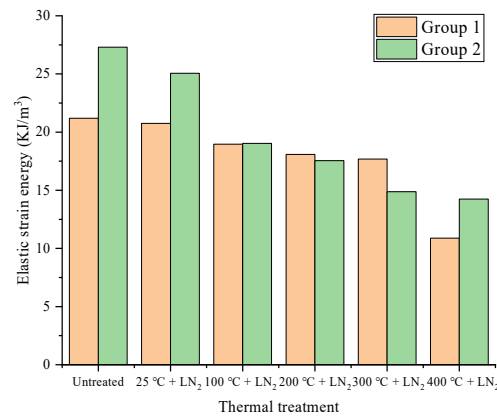


Figure 6. Relationship between temperature and elastic strain energy.

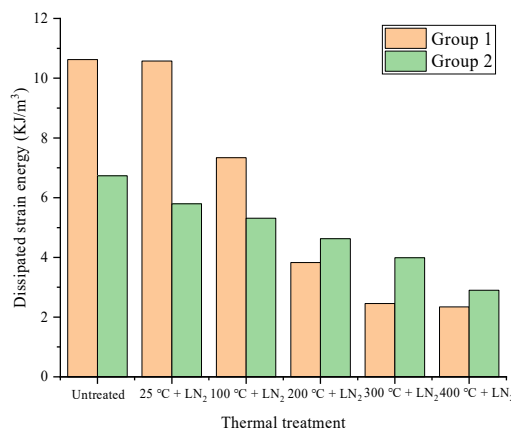


Figure 7. Relationship between temperature and dissipated strain energy.

According to the relevant classification criteria for rock burst proneness, this section categorizes rock burst proneness into four levels: when the *W* value of the rock is greater than or equal to 5, it can be classified as having a strong rock burst proneness; when the *W* value is between 3.5 and 5, it can be classified as having a moderate rock burst proneness; when the *W* value is between 2 and 3.5, it can be classified as having a weak rock burst proneness; and when the *W* value is less than 2, it can be classified as having no rock burst proneness, according to the classification criteria. The trend of rockburst propensity with changes in temperature is shown in Figure 8.

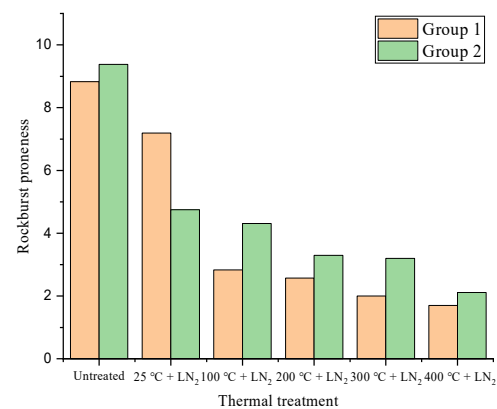


Figure 8. The variation of rock burst tendency with temperature.

The higher rock burst proneness observed in rock samples treated with liquid nitrogen is likely due to the increased internal cracking caused by the cooling process. The presence of these cracks makes the rock more susceptible to fragmentation and failure under stress, leading to a higher likelihood of rock burst occurrence. This effect is further exacerbated at higher temperatures, where the thermal shock induced by the cooling treatment can cause more severe internal damage to the rock. These findings emphasize the significance of assessing the potential risks associated with rock burst incidents when using liquid nitrogen treatment in the mining and construction industries. It is crucial to conduct accurate assessments of the mechanical characteristics of rocks subjected to different cooling techniques and to develop effective strategies for mitigating the risk of rock burst. In addition, it may be necessary to consider alternative cooling methods that can achieve the desired effects without significantly increasing the risk of rock burst. Overall, while liquid nitrogen treatment has been shown to induce significant changes in the mechanical properties of rock samples, its use must be carefully evaluated to minimize potential safety hazards. Further research is necessary to gain a complete understanding of the underlying mechanisms responsible for the observed effects and to develop more effective strategies for enhancing the performance and safety of rock materials subjected to different cooling techniques.

4. Ultrasonic Speed Experiment

4.1. The Principle of Ultrasonic Experimental Detection

When it comes to rock mechanics parameters in engineering practice, ultrasonic waves become crucial. The velocity of ultrasonic waves propagating in rock masses depends on various parameters, such as porosity and the type of propagation medium. While the propagation velocity of ultrasonic waves differs in various media, in rock masses with developed fractures, scattering and waveform changes of ultrasonic waves occur due to the presence of cracks. Ultrasonic waves can be classified into several types based on the direction of wave propagation and the vibration direction of particles in the propagation medium. These types include longitudinal waves, shear waves, Lamb waves, and torsional waves. Each type of wave exhibits unique characteristics and is used for specific applications in ultrasonic testing and measurements. Among them, longitudinal waves primarily rely on changes in the volume of the propagation medium to induce pressure changes and propagate. In experiments, the measurement target is often the velocity of ultrasonic waves in granite. Through extensive experimental research, a more comprehensive understanding and mastery of the internal physical characteristics of rocks can be achieved.

4.2. Ultrasonic Testing and Analysis of Experimental Results

All rock samples in the experiment were subjected to three wave velocity tests, and the average wave velocity at two temperatures was calculated based on the results obtained, as shown in Figure 9.

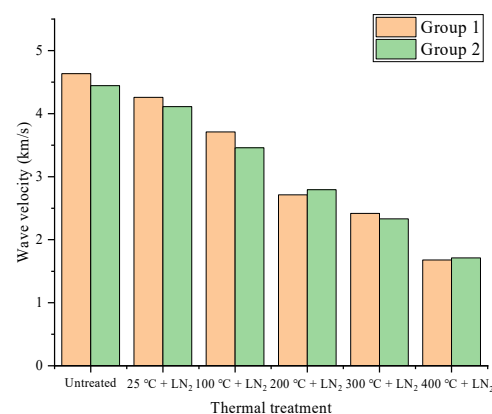


Figure 9. The variation of average wave velocity with temperature.

In the graph, it can be seen that under the same temperature conditions, the rock samples treated with liquid nitrogen have a smaller wave speed than those without liquid nitrogen treatment. Moreover, under the condition of liquid nitrogen cooling treatment, as the treatment temperature increases, the average wave speed tends to decrease, and there is a decreasing trend in which the wave speed becomes faster as the temperature rises. When waves propagate in rocks, they need to pass through the matrix and pores or cracks. The propagation speed in the matrix is much higher than that in the pores or cracks. This indicates that liquid nitrogen treatment will cause freezing damage to rocks, change their strength and ability to resist damage, and increase their cracks, leading to a decrease in wave speed. Different temperatures when all samples are treated with liquid nitrogen can also lead to changes in wave speed. This indicates that as the temperature gets higher, more cracks and larger pores will form inside the rock, and the wave speed will become slower. It can also be seen that the greater the temperature difference during liquid nitrogen treatment, the more obvious the decrease in wave speed. This phenomenon indicates that high-temperature marble, after undergoing liquid nitrogen cooling treatment, undergoes a transformation from a dense and hard brittle structure to a loose and ductile structure. Additionally, this treatment leads to an increase in the number of internal defects and the size of cracks and pores within the marble.

4.2.1. Ultrasonic Time Domain Spectroscopy

The ultrasonic time domain spectrum of rocks is a technique that can naturally reveal the acoustic characteristics of various structures and defects in materials. Its principle is based on the phenomenon of reflection, refraction, and scattering of sound waves as they propagate through different materials at different speeds, thus obtaining the acoustic information of the internal structure of the material. During the process of ultrasonic testing, the ultrasonic wave emitted by the sensor interacts with various structures and defects in the sample while passing through it. Interactions such as multiple reflections, refractions, scatterings, and interference occur when an ultrasonic wave propagates through a sample. These interactions can result in a portion of the wave energy being transmitted back to the sensor. The signal received by the sensor represents the ultrasonic time domain spectrum of the rock.

The ultrasonic time domain spectrum of rocks is a collection of signals composed of the acoustic characteristics of various internal structures and defects, usually presented as pulse reflection signals distributed over a certain period of time in the time domain. Each reflection signal corresponds to the reflection of the ultrasonic wave at the corresponding structure of the sample. Because different structures and defects have different acoustic characteristics, the amplitude, intensity, delay, and other properties of each reflection signal vary. By analyzing the ultrasonic time domain spectrum of rocks, the reflection, refraction, attenuation, and other information of the signal can be comprehensively utilized to identify the location, size, shape, structure, and other features of the rock structure and defects.

Figure 10 shows the ultrasound time domain characteristics. By comparing Figure 10a–d, it can be observed that the ultrasound time domain spectra of the rock samples, which were not treated with liquid nitrogen and subjected to the same temperature, exhibited minimal changes. The reflection images of the ultrasound waves remained uniform, with no significant variations. The dwell time when the amplitude reached its peak was relatively consistent, and the intervals between each reflection form were also relatively uniform.

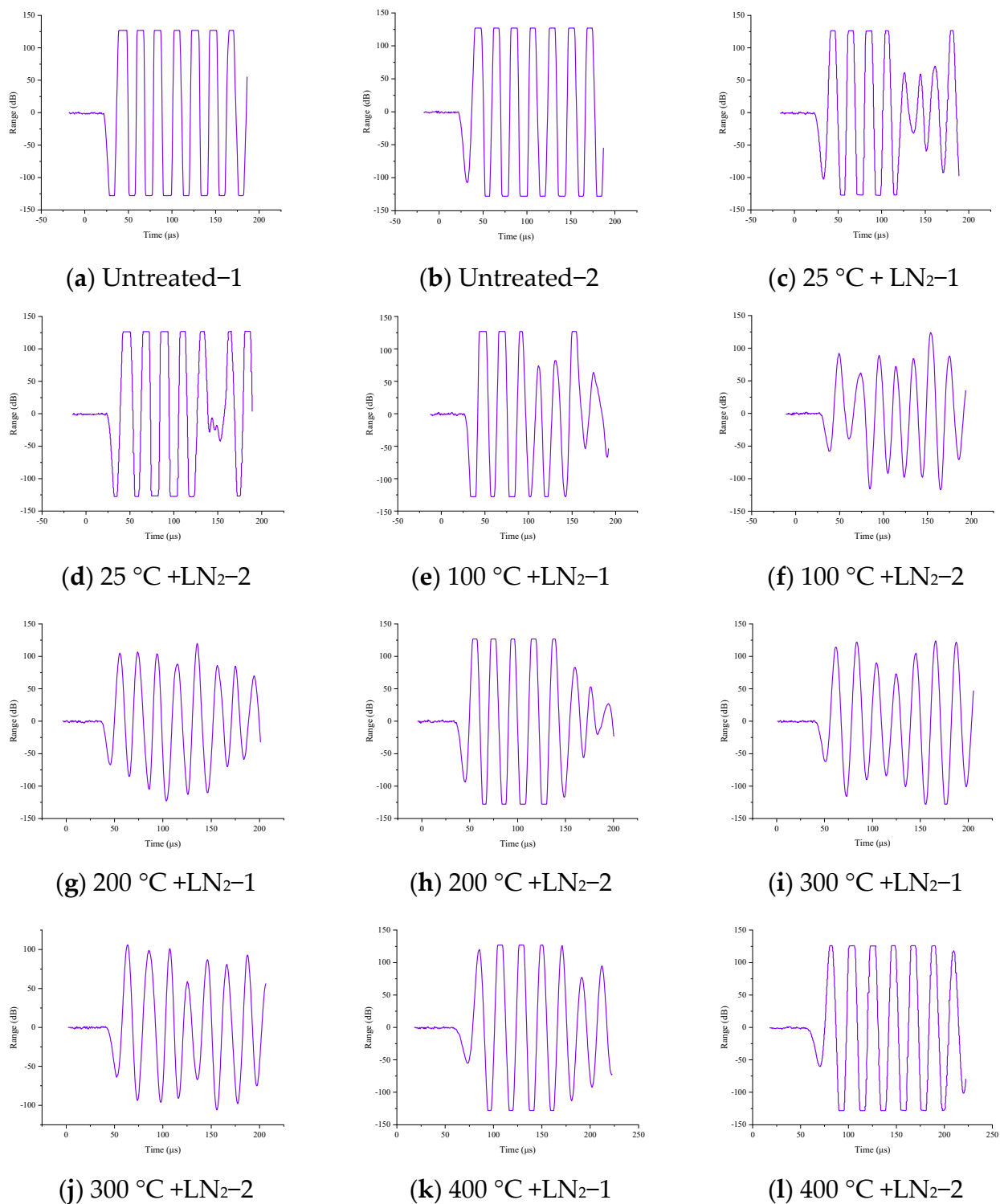


Figure 10. Ultrasound time domain diagram.

However, for the rock samples that underwent liquid nitrogen cooling treatment under room temperature conditions, the initial part of the waveform image resembled that of the untreated rock samples. But as time progressed, particularly around 150 μs , the images underwent drastic changes. This phenomenon was observed in both group 1 and group 2. During this time period, the amplitude of the ultrasound wave decreased, the slope of the reflection wave steepened, the dwell time in the peak amplitude region shortened, and the edges of the images became sharper. The amplitude decayed non-linearly to 50 dB. This

indicates that the internal fractures and voids of the rock underwent changes due to the liquid nitrogen treatment, resulting in variations in the size of the internal rock structure. These changes primarily occurred in the middle section of the rock.

Figure 10 reveals that the images at 100 °C and 200 °C are unstable. The entire process image of these two images became sharper, and the peak amplitude changes were irregular, with unstable slope changes and high degrees of non-linearity. Only a few images had a peak value of 125 dB. This indicates that the internal structure of the rock is chaotic at temperatures between 100 °C and 200 °C, and the level of damage inside the rock is inconsistent. In contrast, the images between 300 °C and 400 °C become more stable compared to the samples treated with liquid nitrogen as stable nonlinearity, slope, and peak dwell time increases. This suggests that the degree of internal damage to the rock samples tends to be consistent when subjected to different temperature differences.

Compared with untreated rock samples at 25 °C, the peak value did not change, but the dwell time decreased, indicating that temperature differences and liquid nitrogen both affect the internal structure of the rock.

4.2.2. Ultrasonic Spectrum

The frequency domain spectrum of ultrasound refers to the representation of ultrasound signals in the frequency domain, which is typically obtained using spectrum analysis methods. Spectrum analysis involves decomposing a signal into different frequency components to obtain its representation in the frequency domain. The spectrum of ultrasound signals in the frequency domain typically displays the intensity and frequency distribution of ultrasound in different frequency ranges. Utilizing ultrasound frequency domain spectrum analysis can assist in detecting defects and material characteristics within objects. As shown in Figure 11, different temperature ranges correspond to different frequency ranges. For example, in material testing, by examining the reflected waves of ultrasound at different frequencies, defects and material properties within the material can be detected. By employing the principles of Fourier transform and programming in MATLAB R2023b, the ultrasound time domain signal of a rock sample can be processed to obtain the frequency domain signal, enabling signal analysis in the frequency domain.

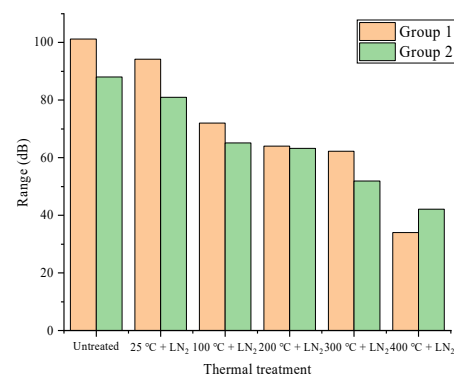


Figure 11. Master frequency amplitude.

Comparing the graphs in Figure 12, it is observed that the main frequencies all occur around 12.5 kHz, exhibiting multiple sharp peaks and waveforms, reflecting a narrow pass band and narrow bandwidth corresponding to the superimposed signals. The low-frequency components of the initial wave are relatively minimal. When compared with samples treated with liquid nitrogen, it is noted that there is no significant deviation in the main frequency. However, a change in the sharpness of the small peaks around 25 kHz is observed. After 50 kHz, there is almost no discernible signal. Upon comparison within the samples, it is found that the processed signal in group 1 has a maximum amplitude of 65 dB, while the unprocessed sample has a maximum amplitude of 100 dB. In group 2, the unprocessed and processed samples have maximum amplitudes of 85 dB and

35 dB, respectively. The comparison within both samples shows a decrease in the maximum amplitude, indicating that liquid nitrogen affects the internal structure of the rock, leading to signal attenuation.

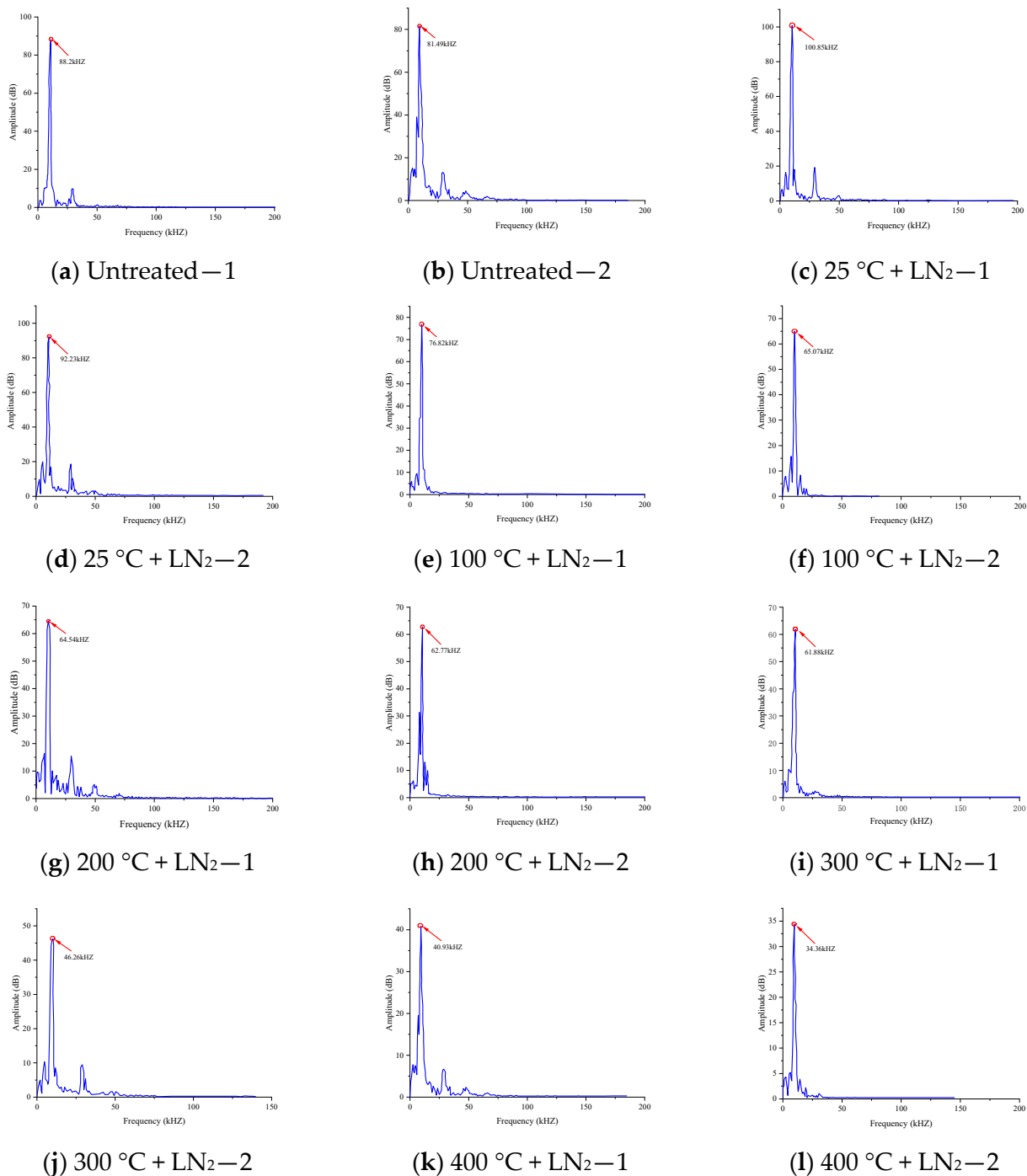


Figure 12. Ultrasonic frequency domain diagram.

It is observed that the ultrasonic frequency spectrum of the treatment of rock samples with liquid nitrogen can induce changes in their properties as a result of the extreme temperature. The same characteristic is seen in the main frequency, which remains around 12.5 kHz and does not deviate with increasing temperature. It can be seen that the image in group 1 has only one main frequency peak, with other small peaks not being very prominent. As the temperature increases from 25 °C to 400 °C, the maximum peak value of

the main frequency in group 1 changes to 65 dB, 75 dB, 35 dB, 90 dB, and 65 dB, respectively, showing different degrees of variation. In group 2, not only is there a main frequency peak at 12.5 kHz, but there is also a small peak at 25 kHz. The maximum peak value of the main frequency changes with temperature from 25 °C to 400 °C as follows: 80 dB, 40 dB, 65 dB, 65 dB, and 90 dB. In particular, in group 2, the images of the rock samples with the smallest main frequency peak values at 200 °C and 300 °C show small peaks that tend to be flat, indicating that changes in temperature gradient also have significant effects on the transmission of signals within the rock samples.

5. Cross-Sectional Scanning

5.1. Principle and Purpose of Cross-Sectional Scanning

Scanning of rock fracture surfaces is a commonly used high-precision detection tool in the field of rocks. Its purpose is to study and analyze the microstructure, rock composition, mineral combination, rock deformation, and metamorphism of rock samples (including actual sampling and artificially prepared samples) by scanning and analyzing the fracture surface of the samples. The significance lies in revealing the structural characteristics of rocks. The scanning of rock fracture surfaces can intuitively observe the microstructure of rocks, such as crystal morphology, grain size, and crystal face orientation, thus revealing the structural characteristics of rocks. It can also analyze the composition and metamorphic degree of rocks by observing characteristics such as particles, mineral combinations, and deformation degree, providing an important basis for the study and exploration of rocks. It can be used to study the mechanical properties of rocks, such as water content, hardness, and disintegration, as well as tensile, compressive, and shear resistance.

5.2. Study on the Characteristics of Granite Sections

As shown in Figure 13, it is a scanned image of the rock cross-section. The irregularity and complexity of the shape of the image section can be analyzed using MATLAB software to process the image section and apply geometric theory. In this paper, the box counting method is a mathematical technique used to calculate the surface fractal dimension of an object. The principle of the box counting method involves dividing an image of size $M \times N$ into smaller $k \times k$ sub-blocks. The grayscale value at position (x,y) in the image is denoted as $f(x,y)$, and the total number of grayscale levels is L . The image can be viewed as a surface grayscale set $(x,y,f(x,y))$ of a three-dimensional object. The XY plane forms a $k \times k$ grid, and the Z-axis represents the grayscale values of the pixels within each grid. Each grid contains several boxes, and the height of each box is as follows:

$$h = (L - 1) \times k / \min(M, N) \quad (2)$$

$$n_r = (i, j) = l - m + 1 \quad (3)$$

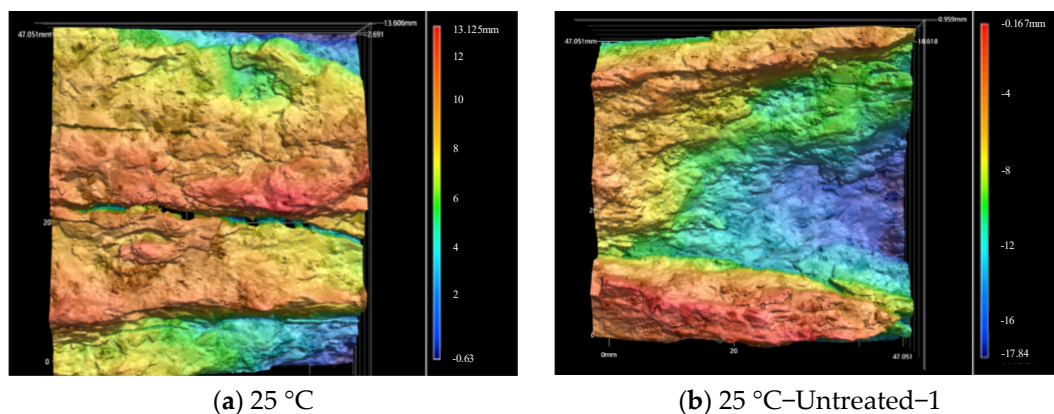


Figure 13. Cont.

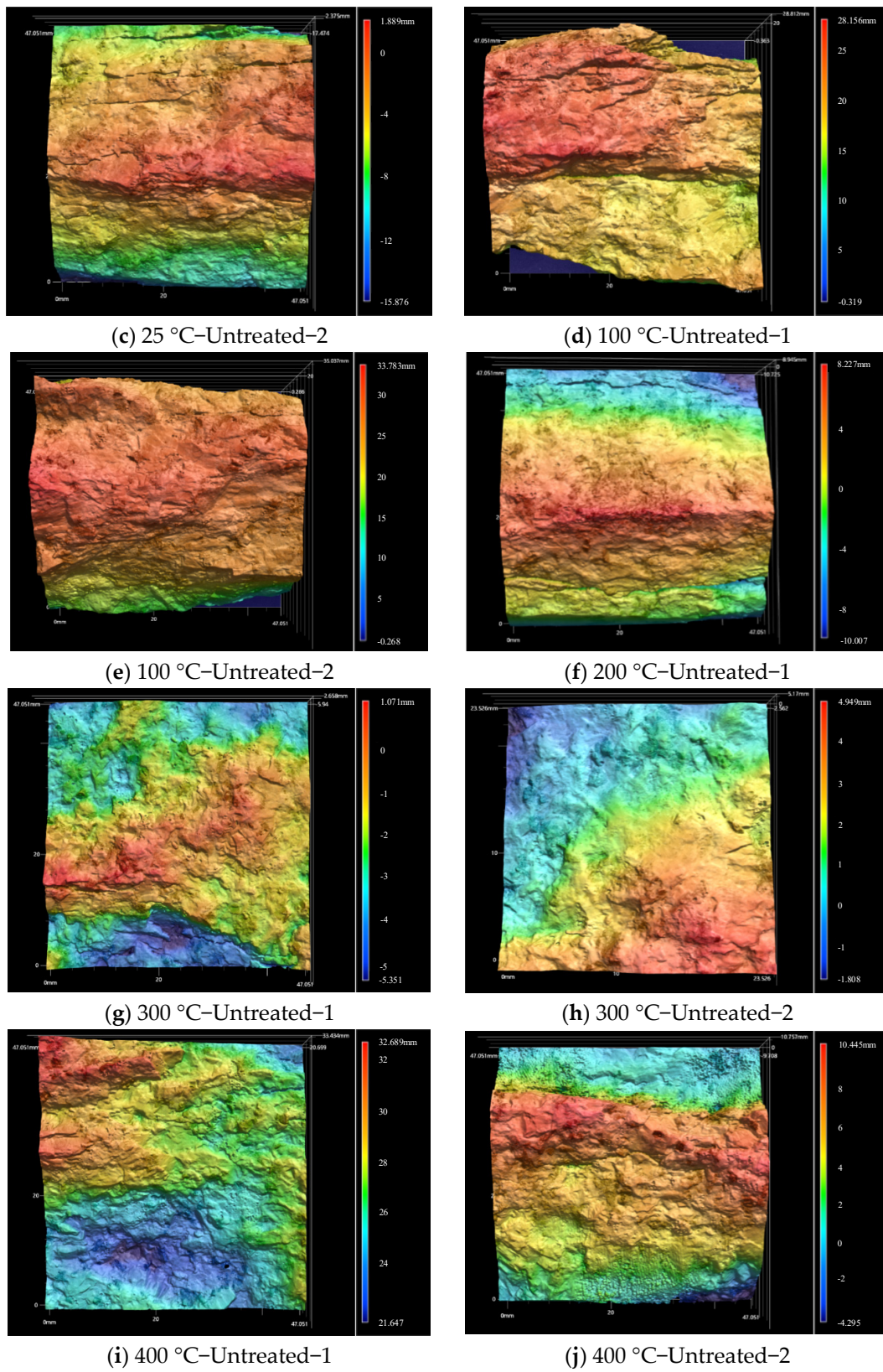


Figure 13. Sample sections at different temperatures.

The total number of boxes covering the entire area is denoted as N_r

$$N_r = \sum_{i,j} n_r(i,j) \quad (4)$$

Based on the given information, the fractal dimension D can be calculated as follows:

$$D = \lim_{r \rightarrow 0} \frac{\log(N_r)}{\log(l/r)} \tag{5}$$

Then, calculate the linear regression of the point pairs $\{\log(1/r), \log(N_r)\}$. The final figure is shown in Figure 14.

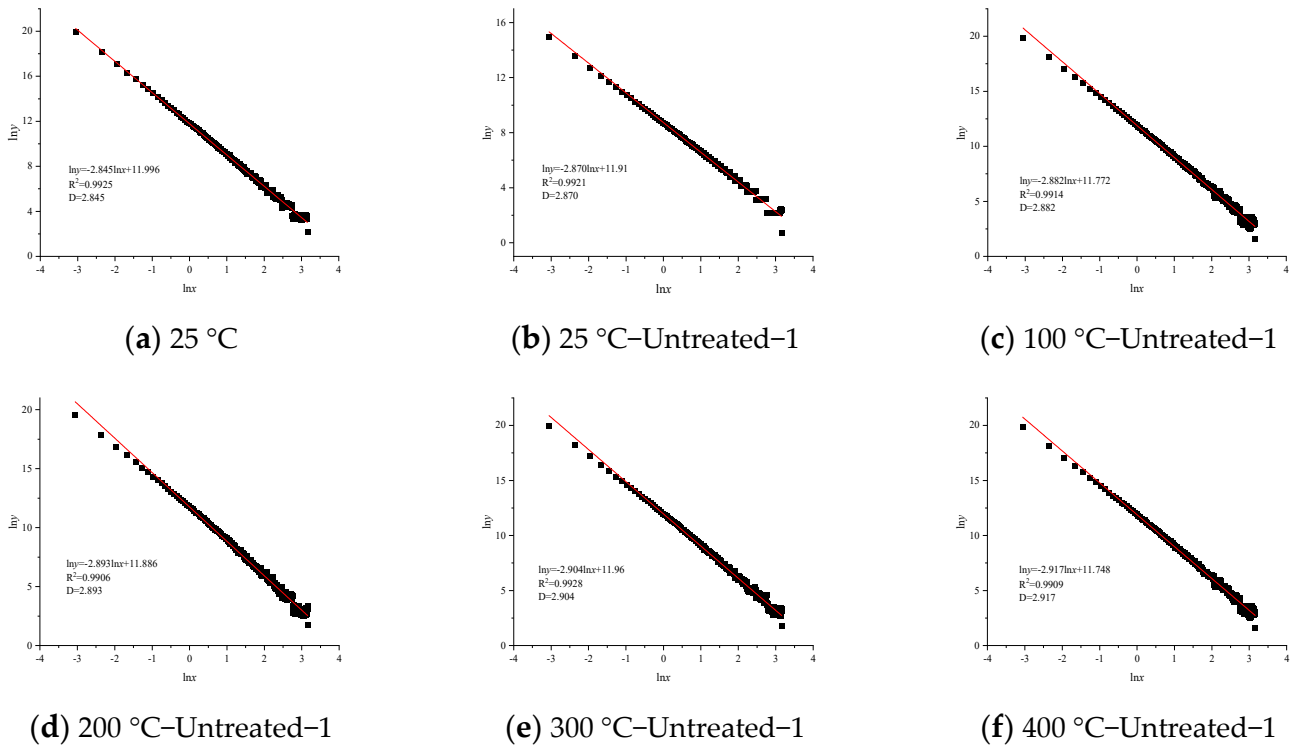


Figure 14. The fitting results of $\ln x$ and $\ln y$ for the corresponding three-dimensional cross-sections of the granite before and after treatment.

Figure 15 shows the box dimension, roughness, and height difference of the cracked surface of granite after high-temperature liquid nitrogen treatment. According to the data in Figure 15, it can be concluded that liquid nitrogen treatment has an impact on the morphological characteristics of the specimens, leading to increased internal cracks and decreased pore width. More specifically, the fractal dimension of the samples increases after liquid nitrogen treatment, indicating that the surface morphology becomes more complex. In contrast, the samples treated with liquid nitrogen exhibit more irregular and rough features. Further observation in Figure 15a reveals that as the temperature increases, the fractal dimension of both Sample 1 and Sample 2 gradually increases. The evolution of characteristic parameters in Figure 15b,c shows a positive correlation between fractal dimension and roughness and height difference. This implies that liquid nitrogen treatment leads to a more uneven and rugged fracture surface, resulting in an increased contact area between the crack network and the matrix. It indicates liquid nitrogen treatment can improve the distribution of damage in granite and increase the extent of damage in the rock mass. In addition, the complexity of granite fractures is enhanced, forming a more intricate crack network. This phenomenon improves gas exchange efficiency and has a positive effect on the processing and utilization of granite. It should be noted that increasing temperature differences will accelerate the growth rate of the fractal dimension. In other words, as the temperature difference increases, the impact of liquid nitrogen treatment on the fracture surface morphology of the rock mass will become more significant. Furthermore, when external forces act on the fracture surface, additional damage can influence the propagation

of cracks. This increases the complexity of the fracture surface and enhances the randomness of the sample. It is worth mentioning that this is consistent with the previously mentioned ultrasonic measurement results, emphasizing the significant impact of liquid nitrogen treatment on the surface properties of the rock mass.

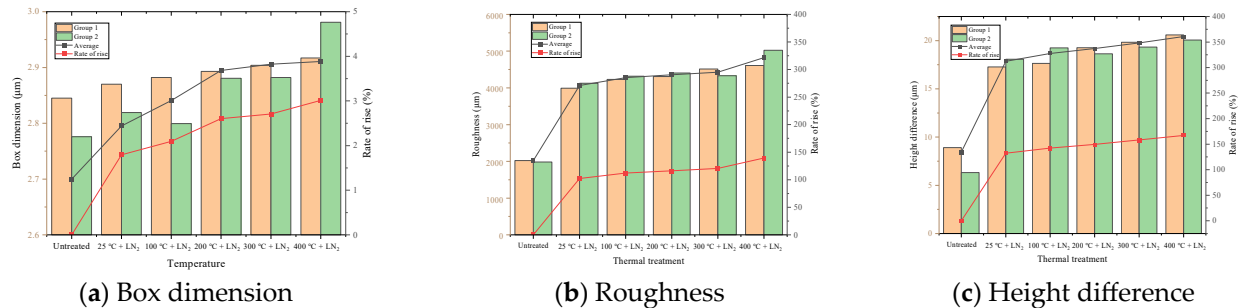


Figure 15. Evolution patterns of characteristic parameters of the fracture surface.

6. Conclusions

- (1) In this study, a comparative analysis was conducted on rock specimens subjected to liquid nitrogen treatment and untreated specimens using uniaxial compression experiments to investigate their mechanical properties. The results revealed distinct differences in the stress–strain behavior between the treated and untreated samples during the compaction stage. Specifically, the stress–strain curve of the treated samples exhibited a faster growth rate and higher hardness compared to the untreated samples. Furthermore, the compressive strength of the specimens exhibited a greater variation with temperature, with a more pronounced change as the temperature increased. Additionally, the elastic modulus of the samples generally exhibited a decreasing trend with temperature, and the rate of change intensified with temperature differences. Moreover, the failure characteristics of the rock specimens subjected to liquid nitrogen treatment shifted from brittle failure to ductile failure. This indicates that the mechanical properties of the rock samples underwent adaptive changes as a result of the liquid nitrogen treatment, potentially attributed to significant alterations in the sample's structure and porosity. Additionally, significant changes in the deformation characteristics of the rock samples during the compression process were observed after the liquid nitrogen treatment. The treatment increased the porosity within the rock, leading to the development of microcracks and fractures, and enhanced the susceptibility to rock burst induction, thereby increasing the likelihood of rock burst occurrence.
- (2) It was observed that the wave velocity of rock samples decreased significantly with increasing temperature, resulting in a relative decrease compared to the original samples. The ultrasonic time domain spectrum indicated that as the temperature rose, the waveform became chaotic, and the duration of the highest value decreased, accompanied by sharper peaks. However, after reaching 300 °C and 400 °C, the waveform smoothed out again. In the ultrasonic frequency domain spectrum, the amplitude of the main frequency changed with temperature, and the sharpness of the wave peaks varied as well. These findings suggest that the signal propagation path within the rock was altered, implying significant changes in the internal structure of the rock due to the influence of liquid nitrogen.
- (3) Cross-sectional scanning of the rock revealed that the use of liquid nitrogen treatment resulted in a more uniform block size distribution in the rock samples, greatly enhancing their ability to undergo volume fracturing. Simultaneously, as the temperature increased, the fracture surface morphology evolved faster, increasing the adsorption and desorption capacity of gas within the cubic rock matrices. Liquid nitrogen treatment also amplified the number of microcracks and led to phenomena such as fragmentation and spalling under external forces. The cross-sectional anal-

ysis of rock scanning is consistent with the findings derived from the experiments mentioned above.

Author Contributions: Conceptualization, Y.C., Y.M. and T.T.; methodology, L.W. and Z.C.; data curation, Y.X. and Z.Z. All authors have read and agreed to the published version of the manuscript.

Funding: The authors are grateful to the financial support from the Scientific and Technological Research Platform for Disaster Prevention and Control of Deep Coal Mining (Anhui University of Science and Technology) (No. DPDCM2207) and the School-Enterprise Collaborative Innovation Fund for graduate students of Xi'an University of Technology.

Data Availability Statement: The data used to support the findings of this study are included within the article.

Conflicts of Interest: The authors declare no conflict of interest.

References

- Li, X.; Chen, D.; Fu, J.; Liu, S.; Geng, X. Construction and Application of Fuzzy Comprehensive Evaluation Model for Rockburst Based on Microseismic Monitoring. *Appl. Sci.* **2023**, *13*, 12013. [\[CrossRef\]](#)
- Wang, L.; Cao, Z.; Xue, Y.; Zhang, W.; Liu, J.; Zhou, Y.; Duan, C.; Chen, T. Effect of weakening characteristics of mechanical properties of granite under the action of liquid nitrogen. *Front. Ecol. Evol.* **2023**, *11*, 1249617. [\[CrossRef\]](#)
- Hong, C.; Yang, R.; Huang, Z.; Qin, X.; Wen, H.; Cong, R.; Liu, W.; Chen, J. Fracture initiation and morphology of tight sandstone by liquid nitrogen fracturing. *Rock Mech. Rock Eng.* **2022**, *55*, 1285–1301. [\[CrossRef\]](#)
- Mao, H.; Xu, N.; Li, X.; Li, B.; Xiao, P.; Li, Y.; Li, P. Analysis of rock burst mechanism and warning based on micro seismic moment tensors and dynamic Bayesian networks. *J. Rock Mech. Geotech. Eng.* **2023**, *15*, 2521–2538. [\[CrossRef\]](#)
- Kocharyan, G.; Qi, C.; Kishkina, S.; Kulikov, V. Potential triggers for large earthquakes in open-pit mines: A case study from Kuzbass, Siberia. *Deep Undergr. Sci. Eng.* **2022**, *1*, 101–115. [\[CrossRef\]](#)
- Zhou, J.; Zhang, Y.; Li, C.; He, H.; Li, X. Rock burst prediction and prevention in underground space excavation. *Undergr. Space* **2023**, *14*, 70–98. [\[CrossRef\]](#)
- Klammer, A.; Peintner, C.; Gottsbacher, L.; Biermann, J.; Bluemel, M.; Schubert, W.; Marcher, T. Investigation of the Influence of Grain-Scale Heterogeneity on Strain burst Proneness Using Rock-Like Material. *Rock Mech. Rock Eng.* **2022**, *56*, 407–425. [\[CrossRef\]](#)
- Yang, X.; Yan, Z.; Bu, S.; Li, W.; Su, C.; Wang, X.; Liu, X.; Yu, N.; Wang, G. Performance analysis, multi objective optimization and working fluid selection for a DPORC system with geothermal source shunting. *Therm. Sci. Eng. Prog.* **2024**, *47*, 102267. [\[CrossRef\]](#)
- Khanmohammadi, S.; Musharavati, F.; Khan, M.S. Proposal a new hybrid system comprising of LNG regasification and geothermal sources: Exergy, exergo-economic, and optimization. *Sustain. Energy Technol. Assess.* **2023**, *60*, 103525. [\[CrossRef\]](#)
- Chen, G.; Sun, Y.; Xu, Z.; Li, X. Hydrogeological feasibility of mine water deep geological storage in Baotashan coarse sandstone: A case study in Ordos Basin. *Deep Undergr. Sci. Eng.* **2022**, *1*, 148–164. [\[CrossRef\]](#)
- Pytel, W.; Fuławka, K.; Pałac-Walko, B.; Mertuszka, P. Numerical and Analytical Determination of Rock burst Characteristics: Case Study from Polish Deep Copper Mine. *Appl. Sci.* **2023**, *13*, 11881. [\[CrossRef\]](#)
- Cai, W.; Dou, L.; Zhang, M.; Cao, W.; Shi, J.Q.; Feng, L. A fuzzy comprehensive evaluation methodology for rock burst forecasting using microseismic monitoring. *Tunn. Undergr. Space Technol.* **2018**, *80*, 232–245. [\[CrossRef\]](#)
- Tai, L.; Li, C.; Gu, S.; Yu, X.; Xu, Z.; Sun, L. Research on dynamic response characteristics of normal fault footwall working face and rock burst prevention technology under the influence of the gob area. *Sci. Rep.* **2023**, *13*, 18676. [\[CrossRef\]](#) [\[PubMed\]](#)
- Lu, Y.; Jiang, N.; Wang, C.; Zhang, M.; Kong, D.; Pan, H. Stability analysis of settled goaf with two-layer coal seams under building load-A case study in China. *Geomech. Eng.* **2023**, *32*, 245.
- Jiang, N.; Lv, K.; Gao, Z.; Di, H.; Ma, J.; Pan, T. Study on Characteristics of Overburden Strata Structure above Abandoned Gob of Shallow Seams—A Case Study. *Energies* **2022**, *15*, 9359. [\[CrossRef\]](#)
- Gu, S.C.; Wang, P.; Yang, C.F. Critical Softening Radius of a Development Heading Causing Rock Bursts. *Int. J. Geomech.* **2023**, *23*, 04023226. [\[CrossRef\]](#)
- Waqar, M.F.; Guo, S.; Qi, S. A comprehensive review of mechanisms, predictive techniques, and control strategies of rock burst. *Appl. Sci.* **2023**, *13*, 3950. [\[CrossRef\]](#)
- Liu, Y.; Wang, G.; Zhu, X.; Li, T. Occurrence of geothermal resources and prospects for exploration and development in China. *Energy Explor. Exploit.* **2021**, *39*, 536–552. [\[CrossRef\]](#)
- Hu, L.; Ju, M.; Zhao, P.; Li, X. Deformation characteristics and novel strain criteria of strainbursts induced by low-frequency cyclic disturbance. *Deep Undergr. Sci. Eng.* **2023**, *2*, 52–60. [\[CrossRef\]](#)
- Qiu, N. Special Collection: Advances of exploration and utilization technology of geothermal resources in China. *Energy Explor. Exploit.* **2019**, *37*, 605–606. [\[CrossRef\]](#)
- Qian, Q.; Lin, P. Safety risk management of underground engineering in China: Progress, challenges and strategies. *J. Rock Mech. Geotech. Eng.* **2016**, *8*, 423–442. [\[CrossRef\]](#)

22. Liu, Y.; Su, X.T. The Formation of Underground Projects Safety and Risk Management Platform. *Appl. Mech. Mater.* **2014**, *584*, 2664–2667. [[CrossRef](#)]
23. Taherkhani, F.; Malmasi, S. Safety risk management based on fuzzy logic at underground projects. *J. Occup. Hyg. Eng.* **2017**, *4*, 49–62. [[CrossRef](#)]
24. Kim, K.M.; Kemeny, J. Effect of thermal shock and rapid unloading on mechanical rock properties. In *ARMA US Rock Mechanics/Geomechanics Symposium; Canada Rock Mechanics Symposium: Asheville, NC, USA, 2009*; p. ARMA-09.
25. Del Greco, O.; Ferrero, A.M.; Oggeri, C. Experimental and analytical interpretation of the behaviour of laboratory tests on composite specimens. *Int. J. Rock Mech. Min. Sci. Geomech. Abstr.* **1993**, *30*, 1539–1543. [[CrossRef](#)]
26. Teng, T.; Li, Z.; Wang, Y.; Liu, K.; Jia, W. Experimental and Numerical Validation of an Effective Stress-Sensitive Permeability Model Under Hydromechanical Interactions. *Transp. Porous Media.* **2024**, 1–19. [[CrossRef](#)]
27. Wu, X.; Huang, Z.; Song, H.; Zhang, S.; Cheng, Z.; Li, R.; Wen, H.; Huang, P.; Dai, X. Variations of physical and mechanical properties of heated granite after rapid cooling with liquid nitrogen. *Rock Mech. Rock Eng.* **2019**, *52*, 2123–2139. [[CrossRef](#)]
28. Sun, F.; Guo, J.; Fan, J.; Liu, X. Experimental study on rockburst fragment characteristic of granite under different loading rates in true triaxial condition. *Front. Earth Sci.* **2022**, *10*, 995143. [[CrossRef](#)]
29. Yin, T.; Ma, J.; Wu, Y.; Zhuang, D.; Yang, Z. Effect of high temperature on the brittleness index of granite: An experimental investigation. *Bull. Eng. Geol. Environ.* **2022**, *81*, 476. [[CrossRef](#)]
30. Cai, C.; Ren, K.; Tao, Z.; Yang, Y.; Gao, F.; Zou, Z.; Feng, Y. Experimental Investigation of the Damage Characteristics of High-Temperature Granite Subjected to Liquid Nitrogen Treatment. *Nat. Resour. Res.* **2022**, *31*, 2603–2627. [[CrossRef](#)]
31. Wang, L.; Xue, Y.; Cao, Z.; Kong, H.; Han, J.; Zhang, Z. Experimental study on mode I fracture characteristics of granite after low temperature cooling with liquid nitrogen. *Water* **2023**, *15*, 3442. [[CrossRef](#)]
32. Cao, Z.; Sun, Q.; Li, Z.; Du, F. Abnormal ore pressure mechanism of working face under the influence of overlying concentrated coal pillar. *Sci. Rep.* **2024**, *14*, 626.
33. Su, Z.; Geng, K.; Zhou, F.; Sun, J.; Yu, H. Influence of freeze-thaw cycles on acoustic emission characteristics of granite samples under triaxial compression. *Adv. Civ. Eng.* **2021**, *2021*, 5571680. [[CrossRef](#)]
34. Kuang, L.; Sun, L.; Yu, D.; Wang, Y.; Chu, Z.; Darkwa, J. Experimental Investigation on Compressive Strength, Ultrasonic Characteristic and Cracks Distribution of Granite Rock Irradiated by a Moving Laser Beam. *Appl. Sci.* **2022**, *12*, 10681. [[CrossRef](#)]
35. Kang, F.; Jia, T.; Li, Y.; Deng, J.; Huang, X. Experimental study on the physical and mechanical variations of hot granite under different cooling treatments. *Renew. Energy* **2021**, *179*, 1316–1328. [[CrossRef](#)]

Disclaimer/Publisher’s Note: The statements, opinions and data contained in all publications are solely those of the individual author(s) and contributor(s) and not of MDPI and/or the editor(s). MDPI and/or the editor(s) disclaim responsibility for any injury to people or property resulting from any ideas, methods, instructions or products referred to in the content.